Functional Materials 19, No.4 (2012)

Geometrization of the temporal photoresponse from the semiconductor sensor materials

V.P.Mygal, A.V.But, O.O.Shmatko, I.V.Bodnar*

National Aerospace University "KhAI",
17 Chkalova Str., 61070 Kharkov, Ukraine
*Belarusian State University of Informatics and Radioelectronics,
6 P. Brovki Str. 220013, Minsk, Republic of Belerus

Received September 9, 2012

Geometrization of the temporal photoresponse of $A^{II}B^{VI}$ semiconductor compounds by means of it transformation to the first- and second-order signatures provides qualitative new possibilities for the control of the compounds quality. It has been offered the integrative indexes of the dynamic and power balances of photoresponse components from sensor crystals which display the basic phases of generation-recombination processes.

Геометризация временного фотоотклика полупроводниковых соединений $A^{II}B^{VI}$ посредством преобразования его в сигнатуры 1-го и 2-го порядков предоставляет качественно новые возможности для контроля качества этих соединений. Предложены интегративные показатели динамической и энергетической сбалансированности составляющих фотоотклика сенсорных кристаллов, которые отображают основные фазы генерационно-рекомбинационных процессов.

1. Introduction

Today quality control problems, as well as monitoring of the production and operation of semiconductor sensors based on the multicomponent solid solutions are far from being solved. This is due to the fact that non-uniformly scaled disorder in the crystalline structure stipulates the multiscale electric field distribution and complex charge transport dynamics in multicomponent semiconductor compounds [1-3]. On one hand the complex dynamics of crystal growth and cooling defines the anomalies in physical properties (photovoltaic, optical, thermal etc.) which are of scientific and practical interest [4]. On the other hand it leads to the ambiguity of the analyzed information and artifacts, which are mainly related to the individual dynamics of photoresponse (PR). In addition, the individual dynamics of PR is associated with the diagnostic problems of semiconductor sensors, as well as their operation in extreme conditions. This makes difficulties for the prediction of the semiconductor sensors performance in extreme conditions, as well as the definition of their capability and quality. As a summary to all mentioned above the further search for methods and tools to identify and analyze the dynamic properties of the sensor materials photoresponse is relevant. Thus, analog signature analysis of dynamic voltage-photocurrent characteristics and PR of sensors based on $A^{II}B^{VI}$ [5, 6] proves quite effective for express control of their operability. In [5], the individuality in PR dynamics was manifested in differential and integral features of PR dynamic structure. Therefore, in our view, to solve the above problems of the materials for semiconductor sensors the interdisciplinary approach is promising [5–7]. It is based on the idea of PR geometrization by converting it into a signature or the wavelet-signature of the phase plane [5, 8]. On one hand the signature configuration displays natural decomposition of temporal PR

onto dynamic components, the character of they distribution in time-frequency domain stipulates the features in dynamics of PR [5, 9]. On the other hand the PR signature encloses an area of the phase plane which can be represented as the power of subset of the dynamic microstates [5]. This allows to analyze the dynamic structure of PR by complementary dynamic and statistical methods [5, 8–10]. Thus, this study aims to further search for the effective methods of identification and analysis of the dynamics of PR from the sensor materials.

2. Experimental

Single crystals of $Cd_{1-x}Zn_xTe$ ($x = 0.05$–0.15) solid solutions were chosen as the model objects of our research. CdZnTe (CZT) crystals are the excellent candidates for use in room temperature hard x- and γ-ray spectrometers. These materials are also of interest for solar cells, medical and space imaging, and find application in nuclear safeguards, transportation security and safety. Therefore, the stability of CZT characteristics is very important. CZT crystals were grown from the melt by the modified Bridgman method of vertical crystallization. Samples had rectangular parallelepiped shape of 6×6×3 mm^3 and 11×11×2 mm^3 in size. The resistivity value of the samples was in a range of $\rho \sim 2 \cdot 10^{10}$–$3 \cdot 10^{11}$ $\Omega \cdot cm$. We employed experimental techniques [9, 11] to investigate the perfection of CZT crystals structure. As a result, the non-uniform spatial distribution of the structural defects was revealed. It caused the multiscale electric field distribution and complex charge transport dynamics in these ternary systems [12]. For these measurements, the surfaces of each crystal were mechanically polished using standard techniques and gold (Au) contacts were deposited on the opposite largest faces of the samples. Photocurrent kinetics was measured in the field with strength of $E = 10$–$2 \cdot 10^2$ V/cm using the electrometric transformer [7]. The light sources were monochromator and LEDs. To detect the "fine" dynamic features the $I(t)$ temporal photocurrent responses were digitized with a sampling frequency of $<10^5$ Hz using ADVANTECH PCI-1711L system of data collection with subsequent processing at a personal computer. Differential geometric parameters of the phase plane signatures were determined using Matlab program package.

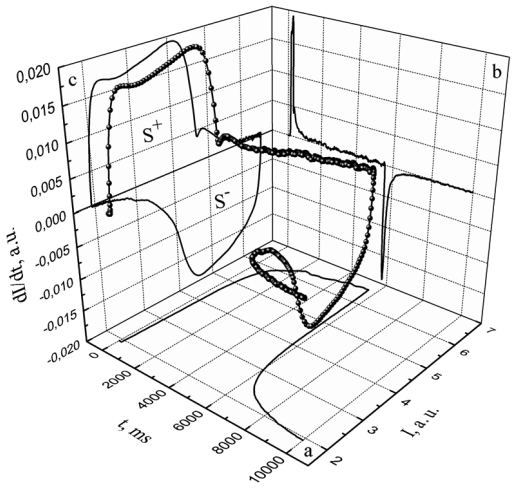

Fig. 1. Dynamical states sequence for CdZnTe crystal in the generalized phase space; dependences: a) $I(t)$; b) $dI/dt = f(t)$ and c) $I(t)$–dI/dt photoresponse signature in the generalized phase space.

3. Results and discussion

Dynamic state of electronic subsystem of the crystal under photoexcitation at a certain time point can be represented by a point in the generalized phase space $dI(t)/dt$–$I(t)$–t (rate-state-time) (Fig. 1). In this case, photocurrent kinetics of CZT crystal (Fig. 1, plane *a*) transforms into a complex trajectory of the dynamical states (Fig. 1, the points on the curve). It conventionally consists of segments which differ in the density of states and, therefore, reflect the dynamic components of PR. These components are clearly visible in the projection of the trajectory of the dynamical states onto the phase plane, which is $I(t)$–dI/dt first-order PR signature (Fig. 1, plane *c*). It should be noted that form of $I(t)$ temporary PR has a various complexity for the different samples. Regardless of this geometric configuration of their $I(t)$–dI/dt signatures is a closed sequence of n segments in the phase plane, which differ in length l, slope $T = d\nu/dx$ and curvature $C = d^2\nu/dx^2$, where $\nu = dI/dt$, and $x = I(t)$. Inherently l, T and C are the differential geometric parameters of dynamic components of the crystal's PR. Partial contributions each of these components are proportional to $I(t)$ axial projection of the corresponding sections. Consequently, as a result of the crystal's PR geometrization through its conversion to $I(t)$–dI/dt signature the natural decomposition of PR onto dynamic components of its structure is realized. Their number and distribution are depend-

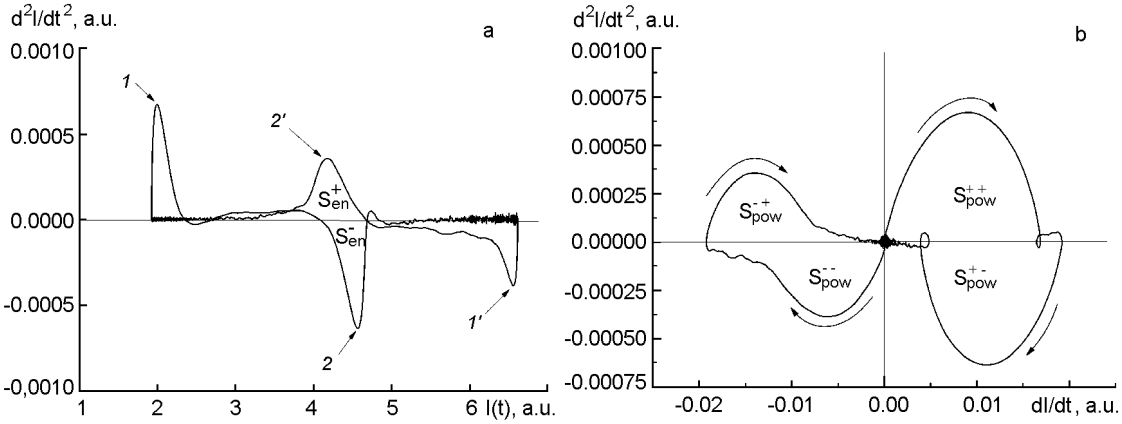

Fig. 2. Second-order photoresponse signatures of CdZnTe crystal.

ent on the quality of the crystals and are individual for each sample.

In addition, the area of $I(t)$–dI/dt PR signature can be represented as power $|W|$ of subset of the dynamic microstates. Their spatial and temporal distribution in the phase plane determines an entropy, since it is proportional to the natural logarithm of W, i.e. $S \sim \ln W$. Statistically entropy indicates the degree of the space-time distribution disorder of dynamic microstates. It was established that rearrangement of the dynamic structure of the crystals' PR after thermal treatment is accompanied by the increment of $dS = dW/W$ entropy. This indicates a decrease in the order and, consequently, in stability of PR. However, after electro acoustic treatment [13] which is coherent with internal factors the decrease of entropy was observed. It indicates an increase in order. The configuration of $I(t)$–dI/dt signature becomes more symmetrical, and photoresponse — more stable. In addition, $B_{dyn} = S^+/S^-$ ratio of the signature areas, which is an indicator of equilibrium distribution of dynamic microstates, tends to 1. Consequently, the individual features of the PR dynamics are integratively displayed in the PR entropy, in its relative change dS/S under the action, as well as in B_{dyn} index of the dynamic states balance. They represent the degree of order in the PR dynamics from different angles. The index B_{dyn} can be used for the outgoing inspection of the sensors manufacturing, as well as for monitoring their performance in extreme conditions.

To identify the energy features of PR dynamics of the sensor materials the second-order signatures are effective [14]. Let us numerically differentiate $I(t)$ dependence twice with respect to time. Now, let us present the time dependence of $I(t)$ state, dI/dt slope and d^2I/dt^2 curvature of PR in the form of the corresponding second-order signatures: $I(t)$–d^2I/dt^2 and dI/dt–d^2I/dt^2 (Fig. 2a, b, respectively). Their areas S_{en} and S_{pow} have the dimensions of energy and power, respectively, which allow to reveal the energy imbalance between the PR components. The most power-consuming PR components are well resolvable in the geometrical configuration of $I(t)$–d^2I/dt^2 second-order PR signature for CdZnTe crystal (Fig. 2a, 1, 2 and 1′, 2′ regions). The area of $I(t)$–d^2I/dt^2 PR signature can be represented as a power of the subset of energy microstates in $\{I(t), d^2I/dt^2\}$ plane. Consequently, the ratio of the areas $B_{en} = S_{en}^+/S_{en}^-$ of the antiphase components of PR separated by $d^2I/dt^2 = 0$ segment (Fig. 2a) shows the energy balance of dynamic components of the PR's structure. It is established that B_{en} index is a function of λ photoexcitation wavelength. Extremes of $B_{en}(\lambda)$ function are in close agreement with the regions of the spectral instability previously identified using $I(\lambda)$–$dI/d\lambda$ parametric spectral signatures of photoresponse [8]. Therefore, $\int_{\lambda_1}^{\lambda_2} B(\lambda)d\lambda$ integral over the photosensitivity region determines the degree of energy imbalance of microstates in the spectral PR. Thus spectral ranges $\Delta\lambda_i$ proper to the extremes of $B_{en}(\lambda)$ are of interest to determine the optimal modes for the combined treatment of the sensors' materials.

It should be noted that the dominant components of PR have both fast and qrelatively slow phases at the photocurrent increase or relaxation (Fig. 2b). For their resolution and spatial-temporal separation we employ transformation of the PR to

dI/dt–d^2I/dt^2 dynamic second-order signature. The configuration of this signature is located in the four quadrants of $\{dI(dt), d^2I/dt^2\}$ plane, which differ in the sign of derivatives (dI/dt and d^2I/dt^2). Obviously, four combinations of the derivatives signs (+ +, + −, − − and − +) indicate the main phases of the generation-recombination processes. Thus in these quadrants dI/dt–d^2I/dt^2 signature enclosed S_{pow}^{++}, S_{pow}^{+-}, S_{pow}^{--} and S_{pow}^{-+} areas which have the dimension of power (Fig. 2b). It should be pointed out that configuration of dI/dt–d^2I/dt^2 signatures is symmetric with respect to abscissa axis and asymmetric with respect to ordinate axis. This allows to analyze dI/dt–d^2I/dt^2 PR signature as a original bicycle in which the sub-cycles of increase and decrease of the rate of change of the photocurrent are spatially separated. Thus B_{pow} index of the power balance of this subcycles is determined from the ratio of their areas $B_{pow} = S_{pow1}/S_{pow2}$, where $S_{pow1} = S_{pow}^{++} + S_{pow}^{+-}$ and $S_{pow2} = S_{pow}^{--} + S_{pow}^{-+}$. It is quite sensitive to external (temperature change etc.) and internal (residual stress etc.) disturbances. At the same time, $d^2I/dt^2 = 0$ segment separates each of subcycle in two conjugated subcycles (Fig. 2b). It allows to split powers of the main phases of the bicycle and to compare them. As a result, $B_{pow} = S_{pow1}/S_{pow2} = 1$ condition for power balance of the sub-cycles of increase and decrease of the rate of change of the photocurrent is implemented with $S_{pow}^{++}/S_{pow}^{--} = S_{pow}^{+-}/S_{pow}^{-+}$ relationship. It shows the ordered distribution of power of the subcycles in opposite phases of bicycle and indicates the presence of dynamic symmetry in the generation-recombination processes. Therefore, this condition can serve as universal criteria of reversibility and stability of the sensor's PR as a dynamical system.

4. Conclusion

Geometrization of the sensor's temporal PR through its presentation in the form of the first- and second-order signatures allows to establish that the PR dynamics are characterized by the spatial and temporal distribution of microstates. On one hand entropy and its relative change dS/S under the action (treatment), as well as the balance of dynamic components of PR represents the degree of order of the dynamic microstates distribution in the phase plane. On the other hand B_{en} index represents the degree of order of the energy microstates distribution in $\{I(t), \{I(t), d^2I/dt^2\}$ plane. In this case, the power balance of the dynamic components $B_{pow} = 1$ in the four phases of the generation-recombination processes can serve as universal criteria of reversibility and stability of the sensor's PR as a dynamical system. In whole, the results of this study indicate that the overall form of organization of responses from different sensor materials is determined by the spatial and temporal ordering of its structure. Therefore, the proposed tools for identifying and analyzing the PR dynamics of sensor materials have the prospect for the quality control of the complex semiconductor compounds [15, 16]. It has been confirmed by the results of the study of PR from ternary compounds $CuIn_5X_8$(X–S, Se, Te) which are characterized by the anisotropic and multiscale character of properties.

This study has been supported by the State Foundation for Basic Research in Ukraine.

References

1. D.J.Fu, J.C.Lee, S.W.Choi et al., *Appl. Phys. Lett.*, **81**, 5207 (2002).
2. R.P.Huebener, K.M.Mayer, J.Parisi et al., *Nucl. Phys. B — Proceed. Supplements*, **2**, 3 (1987).
3. E.Scholl, Cambridge University Press, Cambridge Nonlinear Science Series, No. 10, 2001.
4. V.P.Mygal, A.L.Rvachev, O.N.Chugai, *Fiz. i. Tehn. Polupr.*, **19**, 1517 (1985).
5. A.V.But, V.P.Mygal, A.S.Phomin, *Techn. Phys.*, **57**, 575 (2012).
6. A.V.But, V.P.Mygal, A.S.Phomin, *Semiconductors*, **45**, 153 (2011).
7. A.V.But, V.P.Mygal, A.S.Phomin, *Functional Materials*, **16**, 5 (2009).
8. A.V.But, V.P.Mygal, A.S.Phomin, *Semiconductors*, **43**, 581 (2009).
9. N.G.Kalugin, G.Nachtwei, Yu.B.Vasilyev et al., *Appl. Phys. Lett.*, **81**, 382 (2002).
10. G.Flatgen, R.Richter, A.Kittel et al., *Phys. Lett. A*, **177**, 148 (1993).
11. G.Koley, J.Liu, Krishna C.Mandal, *Appl. Phys. Lett.*, **90**, 102121 (2007).
12. A.L.Washington, L.C.Teague, M.C.Duff et al., *J. Appl. Phys.*, **110**, 073708 (2011).
13. Ukrainian Patent No. 93947 (2011).
14. Ukrainian Patent No. 77203 (2006).
15. K.Kim, D.Chang, S.K.Lim et al., *Current Appl. Phys.*, **11**, 1311 (2011).
16. M.L.Trunov, S.N.Dub, R.S.Shmegera, *Techn. Phys Lett.*, **31**, 551 (2005).

Геометризація часового фотовідгуку напівпровідникових сенсорних матеріалів

В.П.Мигаль, А.В.Бут, О.О. Шматко, І.В.Боднар

Геометризація часового фотовідгуку напівпровідникових сполук $A^{II}B^{VI}$ шляхом його перетворення в сигнатури 1-го і 2-го порядків надає якісно нові можливості для контролю якості цих сполук. Запропоновано інтегративні показники динамічної і енергетичної збалансованості складових фотовідгуку сенсорних кристалів, які відображають основні фази генераційно-рекомбінаційних процесів.